Electronic Supplementary Material (ESI) for Materials Chemistry Frontiers.
This journal is © the Partner Organisations 2020

Electronic Supplementary Information

Zirconium oxide nanoarrays via self-organized anodizing of Al/Zr bilayers on substrates

Alexander Mozalev,[*a,b] Zdenek Pytlicek,[a] Kirill Kamnev,[a] Jan Prasek,[a,b]

Francesc Gispert-Guirado[c] and Eduard Llobet[d]

[a]*CEITEC* – Central European Institute of Technology, Brno University of Technology, Purkynova 123, 61200 Brno, Czech Republic

[b]Brno University of Technology, Faculty of Electrical Engineering and Communication, Department of Microelectronics, Technicka 10, 616 00 Brno, Czech Republic

[c]SRCiT, University Rovira i Virgili, Av. Paisos Catalans 26, 43007 Tarragona, Spain

[d]MINOS, University Rovira i Virgili, Av. Paisos Catalans 26, 43007 Tarragona, Spain

Corresponding author:

Alexander Mozalev

Email: alexander.mozalev@ceitec.vutbr.cz

XRD analysis

The preferred orientation of the phases was corrected with the March-Dollase model.[1,2] This correction was necessary as the samples analysed were in a solid form and some degree of orientation was expected from the deposition process. The TOPAS[3] software allows for this correction up to three independent parameters which are fitted for a maximum of two crystallographic directions. In the high symmetry phases, one crystallographic direction was enough to correct the preferred orientation but with the low symmetry phases two directions were used. We have to admit that the March-Dollase model has not been perfectly good for correcting the preferred orientation for the low symmetry phases, generating a misfit between the observed and the calculated diffractograms with a higher estimated standard deviation (e.s.d.) of the refined preferred orientation parameters. More complex models, like the generalized spherical-harmonic description, GSH,[4,5] have been discarded due to the insufficient resolution of the experimental diffractograms.

Table S1. Summary of the crystallographic parameters for phases refined from the X-ray diffractograms measured for the anodized, re-anodized, air-annealed, and vacuum-annealed samples (as in Figure 6). R_{wp} is the conventional Rietveld agreement factor. The e.s.d. of the last significant digit of calculated parameters is given in parenthesis.

Phase	Space group	ICSD n. ¶	Cell parameters / Å	Crystal. size / nm	Preferred orientation parameter	Relative amount / wt.%
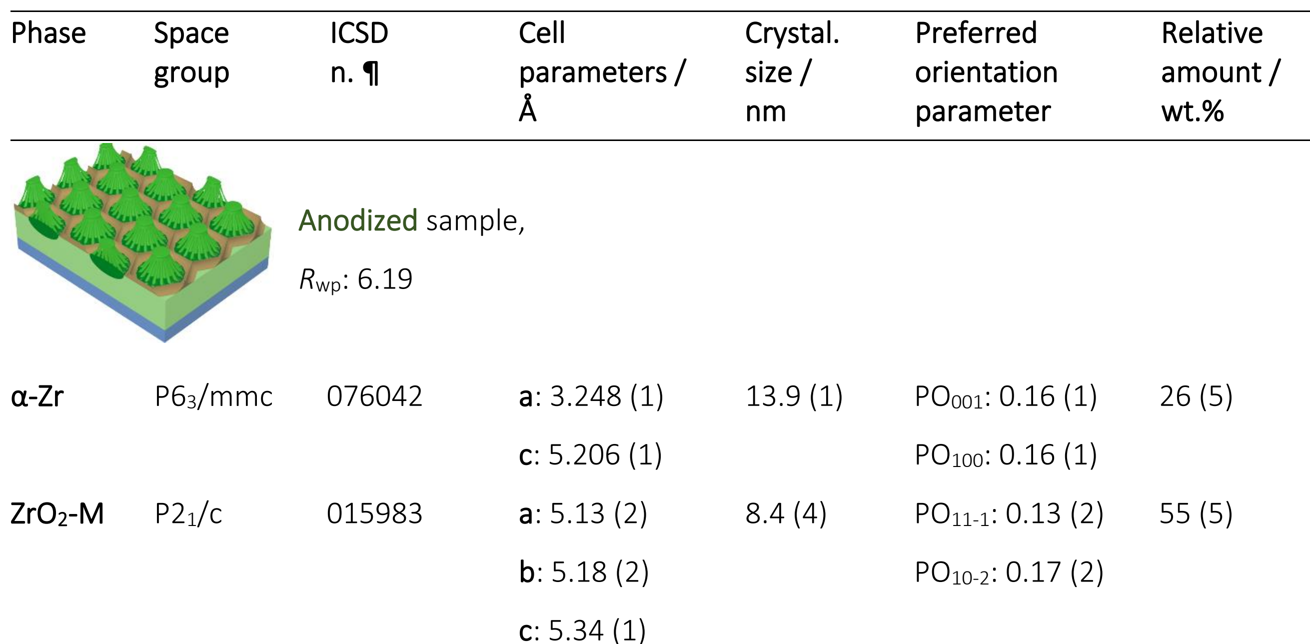		Anodized sample, R_{wp}: 6.19				
α-Zr	$P6_3/mmc$	076042	**a**: 3.248 (1) **c**: 5.206 (1)	13.9 (1)	PO_{001}: 0.16 (1) PO_{100}: 0.16 (1)	26 (5)
ZrO_2-M	$P2_1/c$	015983	**a**: 5.13 (2) **b**: 5.18 (2) **c**: 5.34 (1)	8.4 (4)	PO_{11-1}: 0.13 (2) PO_{10-2}: 0.17 (2)	55 (5)

			β: 103.7 (4)			
ZrO_2-C	Fm-3m	089429	**a**: 5.180 (2)	6.3 (4)	PO_{111}: 0.2 (1)	14 (3)
Al_3Zr_4	P6/mmm	603486	**a**: 5.499 (6)	12.8 (4)	PO_{2-10}: 0.22 (3)	4 (3)
			c: 5.37			

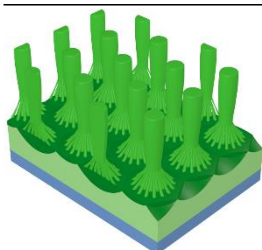

Re-anodized sample,

R_{wp}: 12.2

α-Zr	$P6_3/mmc$	076042	**a**: 3.2441 (2)	1 3.4 (3)	PO_{001}: 0.18 (6)	100
			c: 5.1976 (5)		PO_{100}: 0.19 (1)	

Air-annealed sample,

R_{wp}: 7.30

ZrO_2-M	$P2_1/c$	015983	**a**: 5.150 (6)	7.7 (2)	PO_{001}: 0.1 (1)	100
			b: 5.181 (6)		PO_{10-2}: 0.34 (5)	
			c: 5.340 (1)			
			β: 99.30 (5)			

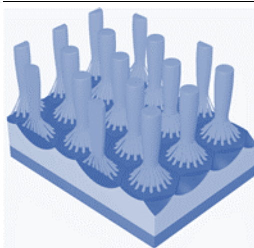

Vacuum-annealed sample,

R_{wp}: 6.01

α-Zr	$P6_3/mmc$	076042	**a**: 3.2513 (3)	16.5 (3)	PO_{001}: 0.22 (1)	31 (4)
			c: 5.2066 (6)		PO_{100}: 0.22 (1)	
ZrO_2-M	$P2_1/c$	015983	**a**: 5.131 (9)	10.3 (5)	PO_{001}: 0.1 (1)	69 (4)
			b: 5.182 (9)		PO_{10-2}: 0.38 (2)	
			c: 5.314 (2)			
			β: 100.25 (1)			

EDS elemental line scan analysis

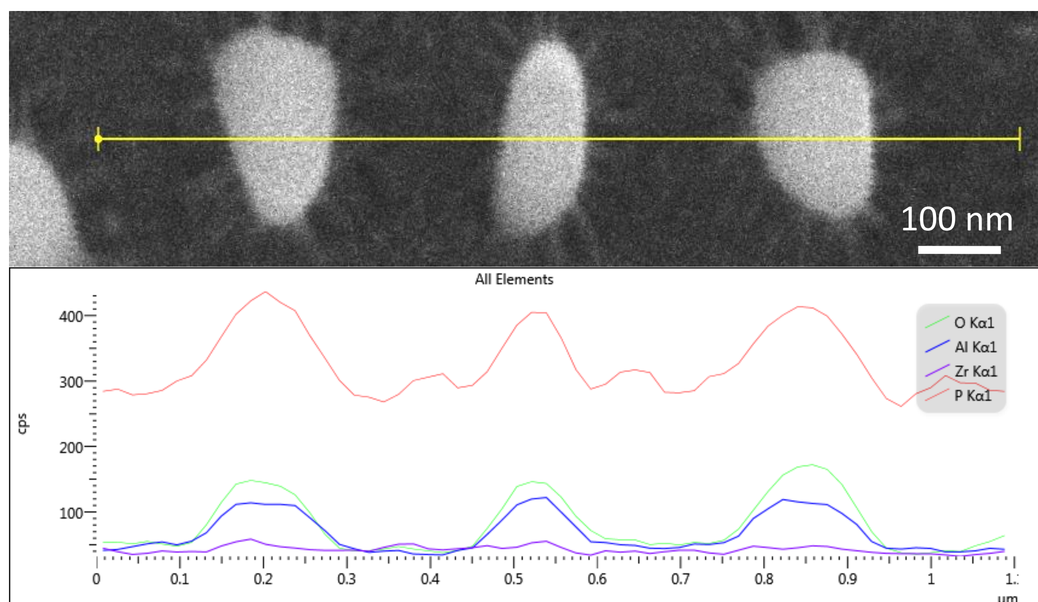

Fig. S1. EDS elemental line scan of the *re-anodized* sample, that is, processed in 0.2 M H_3PO_4 as shown in Fig. 1b and SEM imaged in fig.2). The beam voltage is 15 kV.

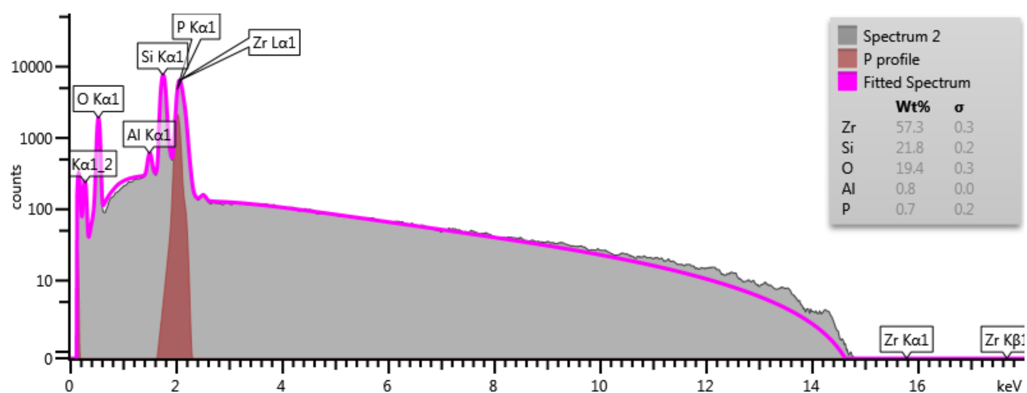

Fig. S2. EDX spectrum of the *re-anodized* sample with the P lines emphasized (the beam voltage 15 kV)

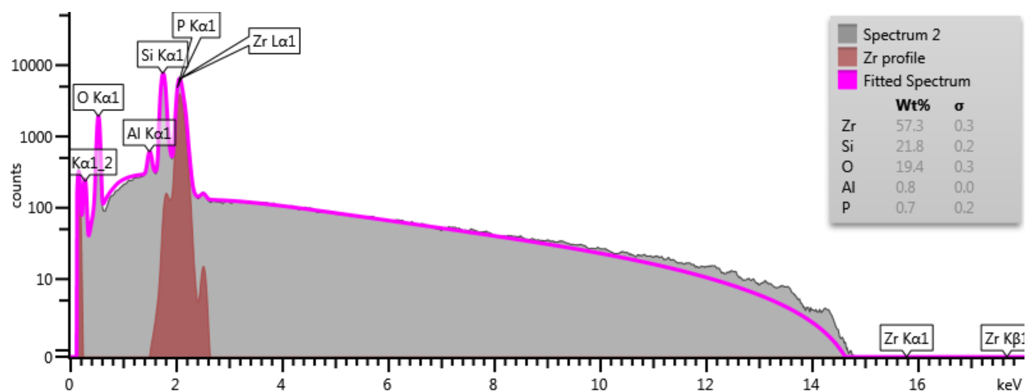

Fig. S3. EDX spectrum of the *re-anodized* sample with the Zr lines emphasized (the beam voltage was 15 kV)

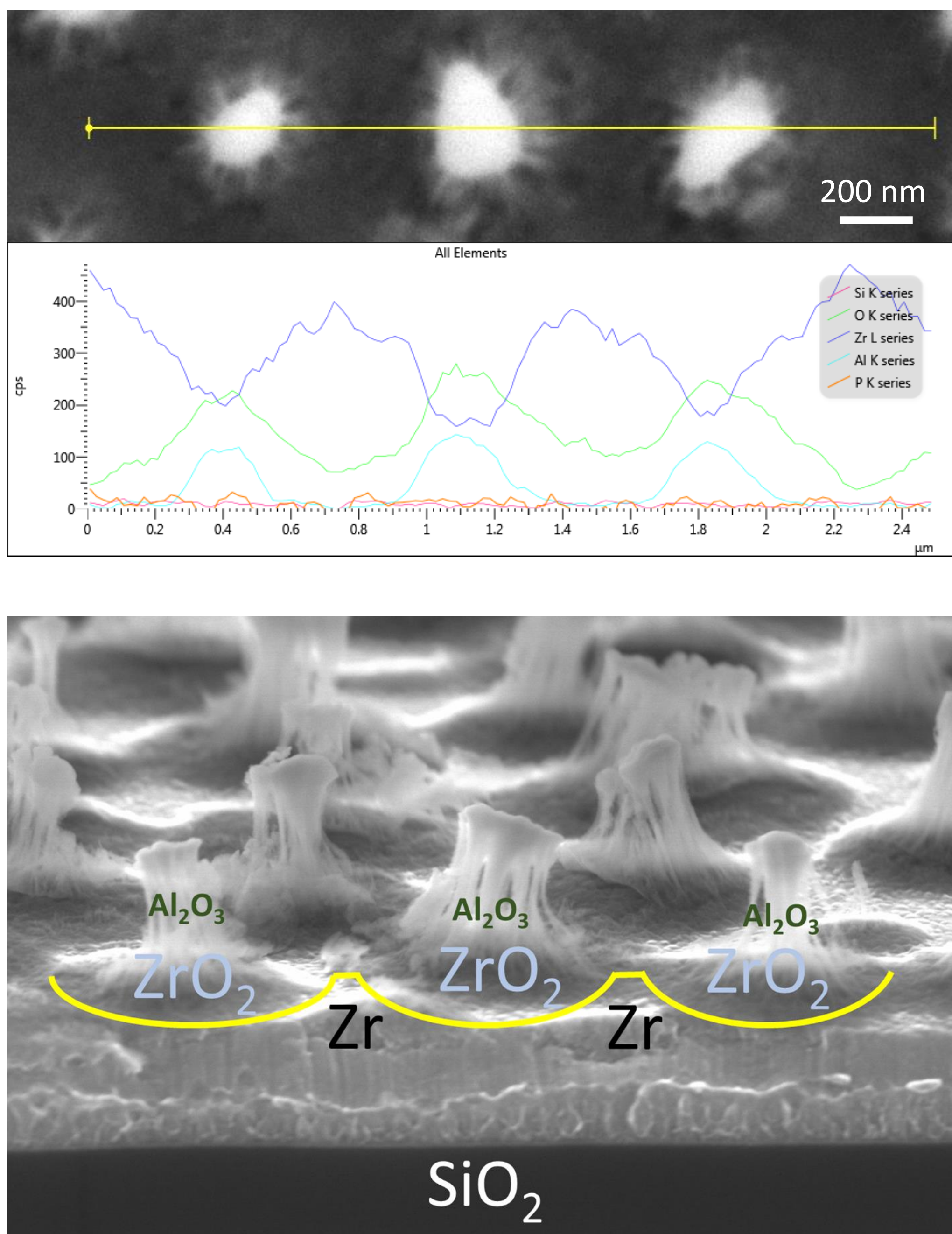

Fig. S4. EDS line scan of the anodized/re-anodized sample prepared in 0.02 M etidronic acid electrolyte at 300/450 V, as shown in Fig. 4e and f of the main text. The beam voltage was 7 kV.

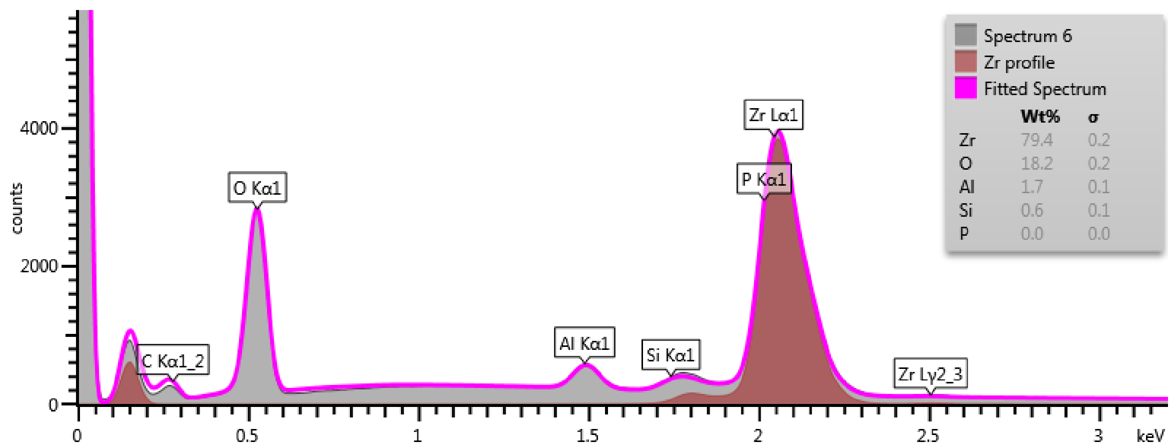

Fig. S5. EDX spectrum of the *etidronic-acid-made* sample (the beam voltage was 7 kV)

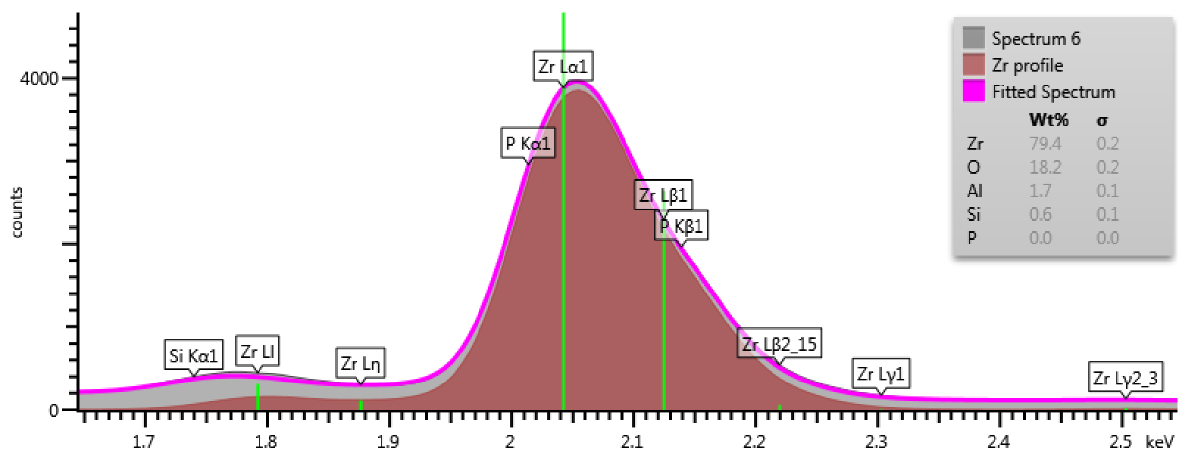

Fig. S6. A cropped portion of the EDX spectrum of Fig. S5 to elaborate the main Zr peak

Interpretation

First, the EDS elemental line scan surface analysis was performed for the re-anodized sample, which was prepared as shown in Fig. 1b and SEM examined in Fig. 3 of the main article. Schematic process for forming this sample is outlined in Fig. 7, the details of the outer and inner profiles are elaborated in Fig. 8. The selected elements were Zr, O, P, and Al.

Fig. S1 shows an SEM image of the sample surface recorded at 15 kV accelerating voltage and the lines of the above elements synchronized with the SEM image. Fig. S2 and S3 show the EDX spectra of this sample emphasizing the positions of P and Zr peaks, respectively. As the P and Zr peaks substantially overlap, the analysis software was not unable to reliably discriminate the Zr line, therefore there is no profile of the Zr line in Fig. S1. Nevertheless, the behaviors of the O, Al,

and P lines correspond well to the interpretation of the element distribution made on the base of the XPS and XRD results. Thus, the alumina is located within the nanopillars but not around them, the same is true for the P-containing species. Obviously, there is an increased amount of oxygen within the pillars since the physical amount of ZrO_2 is obviously bigger compared with the oxide covering the gaps around the pillars. Therefore, **the EDS line scan results reinforce the conclusions made in the main text from the XPS and XRD analyses** and used to model the film structure and composition in Fig. 8.

Additionally to the above experiment, we have made EDS line scan analysis of the nano-hoodoos of sample prepared in the Etidronic acid solution, as shown in Fig. 4e and f of the main text. The difference was not only in the pillar sizes but also in the expected absence of P-species in the oxide and the presence of metallic Zr around the pillars, as described in the main text. Fig. S4 shows an SEM image of the sample surface recorded at 7 kV accelerating voltage and the lines of the above elements synchronized with the SEM image. Fig. S5 and S6 show respectively the whole and cropped EDX spectra of the Etidronic-acid-made sample. Due to the low accelerating voltage, the SiO_2 substrate is practically unaffected by the analysis. Due to the absence of phosphorus, the Zr line is now well resolved showing an increased Zr presence around the hoodoos, while the oxygen and aluminum signals are stronger within the hoodoos. This means that there is much more ZrO_2 inside the hoodoos, the Al_2O_3 is again located within the hoodoos only, and the gaps are much less oxidized relative to the hoodoos. One may see that **the EDS line scan analysis results are again in line with the interpretation and conclusions derived from the SEM, XPS, and XRD results**.

References

1 A. March, Mathematische Theorie der Regelung nach der Korngestalt bei affiner Deformation. *Z. Kristallogr.,* 1932*,* **80**, 285.

2 W. Dollase, Correction of Intensities for Preferred Orientation in Powder Diffractometry: Application of the March Model. *J. Appl. Crystallogr.,* 1986, **19,** 267.

3 TOPAS, v5.0 (Computer Software). *Bruker AXS*. 2011, Karslruhe, Germany.

4 M. Järvinen, Application of Symmetrized Harmonics Expansion to Correction of the Preferred Orientation Effect. *J. App. Cryst.,* 1993, **26,** 525.

5 H. Bunge, *Texture Analysis in Materials Science.* London: Butterworths, 1982.